ISSN: 1231-4005
e-ISSN: 2354-0133
DOI: 10.5604/12314005.1138276

INFLUENCE OF ENGINE LOAD ON PISTON RING PACK OPERATION OF A MARINE TWO-STROKE ENGINE

Andrzej Wolff

Warsaw University of Technology
Faculty of Transport
Koszykowa Street. 75, 00-662 Warsaw, Poland
tel.: +48 22 234 81 13, fax: +48 22 849 03 21
e-mail: wolff@it.pw.edu.pl

Abstract

A set of piston rings is used to form a dynamic gas seal between the piston and cylinder wall. Many physical phenomena are associated with the operation of the system piston-ring-cylinder (PRC), such as: inter-ring gas dynamics for the labyrinth seal, hydrodynamic lubrication and mixed friction in gaps between the rings and cylinder liner, oil flow and distribution of lubricant along the liner, twist motion of rings, liner temperature influence on the oil viscosity.

A complex model of the PRC system has been developed by the author. Among own models it includes several sub-models taken from literature, like: a model of viscous oil flow between rough gap surfaces formulated by Patir & Cheng and an elastic contact model of Greenwood & Tripp.

The main parts of the mathematical model and software have been experimentally verified abroad by the author at the marine engine-designing centre. A relatively good qualitative and quantitative compatibility between the experimental measurements and calculated results has been achieved.

In contrast to the previous papers of the author, new calculation results for a marine two-stroke engine have been presented. These results concern influence of engine load on piston ring pack operation of the analysed engine. They include basic physical quantities associated with gas and oil flow in the piston-ring-cylinder system of the engine.

The developed model can be utilized for: evaluation of gas leakage through the sealing ring set, prediction of lubrication conditions of piston rings and oil consumption, defining areas of the possible cylinder liner wear and profile changes of piston rings sliding surfaces, and thus can be useful for optimization of the PRC system design.

Keywords: *marine engines, piston rings, gasdynamics, hydrodynamic lubrication, mixed friction*

1. Introduction

Piston rings are important part of internal combustion engines. Commonly, a set of piston rings is used to form a dynamic gas seal between the piston and cylinder wall. The sliding motion of the piston forms a thin oil film between the ring land and the cylinder wall, which lubricates the sliding components [2, 4, 10]. The hydrodynamic force generated by this thin oil film is opposed by a combination of the gas force acting on the backside of each ring and the ring stiffness force. Due to the dynamic nature of these forces, each individual ring is periodically compressed and extended as the piston runs through its cycle. The problem of studying this interaction is further complicated by the high temperatures involved, as these result in low oil viscosity and subsequently very low oil film thickness. The oil film is typically thick enough to ensure the existence of mixed lubrication, so that the latter phenomenon should also be taken into account [2, 3, 7, 8, 11]. Numerical simulation of these processes, which take place in a typical piston ring pack operation, is important from practical point of view.

The purpose of this paper is to present numerical calculations of piston ring pack operation for a marine two-stroke internal combustion engine working at part and full load conditions.

2. Modelling of piston ring pack operation

2.1. Developed sub-models

A combined model of piston rings operation has been developed. It consists of two main models: a) model of gas flow through the labyrinth seal piston-rings-cylinder (PRC), b) model of oil flow in the lubrication gap between the ring and cylinder liner. The two mentioned models are coupled. In addition, sub-models of the following mechanical phenomena have been used: a contact of rough surfaces, an axial movement of rings within piston grooves and an elastic torsional deformation of piston rings (Fig. 1).

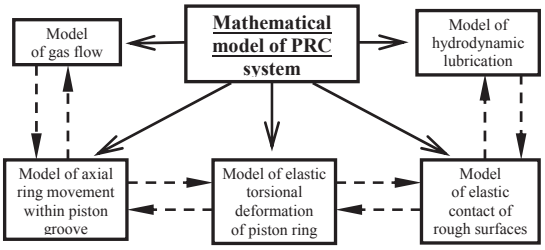

Fig. 1. Developed complex model of the system: piston-ring-cylinder (PRC)

2.2. Model of gas flow through the labyrinth seal of piston rings

The gas flow model [15, 16, 17, 18] consists of several volume regions V_1, V_2, …, V_9, which are connected by orifices with cross-section areas A_1, A_2, …, A_{12} (Fig. 2). The volumes V_3, V_5, V_7 correspond to volumes between the piston rings, while volumes V_2, V_4, V_6, V_8 correspond to groove volumes behind rings. Orifices with cross-section areas A_1, A_4, A_7, A_{10} correspond to the ring end gaps, whereas orifices with cross-sections A_2, A_3, A_5, A_6, A_8, A_9, A_{11}, A_{12} correspond to ring-side crevices.

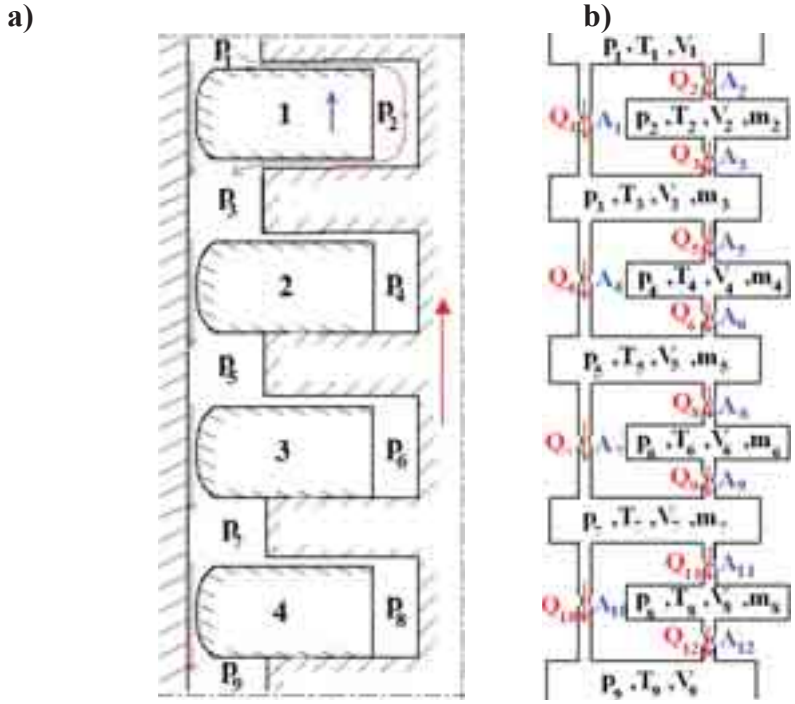

Fig. 2. Scheme of gas flow through the labyrinth seal: a) piston–rings–cylinder system, b) applied physical model for a two-stroke marine engine with four piston rings

It was also assumed that the gas flow through orifices is isentropic (depending on pressure ratio – subsonic or sonic). The heat transfer between gas volume regions and surrounding walls was taken into account.

Thermal expansion of the piston and the cylinder liner and wear of the cylinder liner were taken into account. Leaks between piston rings and cylinder liner were defined by flow areas of ring end gaps, which depend on the position of the piston in cylinder.

In addition, mathematical description takes into account changes of gas volume regions and cross-section areas between the rings and the piston grooves (due to axial movement of the rings) [5, 6, 11, 15-18].

In the mathematical model of these phenomena, equations of the following physical laws are utilized (here given for a gas volume number *k*):

a) equation of mass balance:

$$dm_k = \sum_i dm_{In_i} - \sum_j dm_{Out_j}\,, \tag{1}$$

b) equation of energy balance"

$$\sum_i dm_{In_i} \cdot i_{In_i} - \sum_j dm_{Out_j} \cdot i_{Out_j} - \delta Q_{Wall} = d\left(m_k \cdot u_k\right) + p_k \cdot dV_k\,, \tag{2}$$

c) gas state equation in differential form"

$$dT_k = T_k \cdot \left(\frac{dp_k}{p_k} + \frac{dV_k}{V_k} - \frac{dm_k}{m_k} \right), \tag{3}$$

where:

m – gas mass,
p – gas pressure,
T – gas temperature,
u – internal gas energy,
i – gas enthalpy,
Q – heat transferred through cylinder walls,
In – gas inflow,
Out – gas outflow,
i – number of inflow channel,
j – number of outflow channel,
k – number of gas volume.

2.3. Model of oil flow in a gap (with rough surfaces) between the ring and cylinder

Two main cases of oil flow in the system piston ring – cylinder liner are presented in Fig. 3.

A one-dimensional form of the modified Reynolds equation developed by Patir and Cheng [7, 8] has been used to calculate hydrodynamic forces in the case of rough gap surfaces. This equation is applicable to any general roughness structure and takes the following form:

$$\frac{\partial}{\partial x}\left(\phi_x \frac{h^3}{12\mu} \frac{d\,\bar{p}}{d\,x} \right) = \frac{U}{2} \frac{d\,\bar{h}_T}{dx} + \frac{U}{2} \sigma \frac{d\phi_S}{dx} + \frac{d\,\bar{h}_T}{dt}\,, \tag{4}$$

where:

t – time,
x – coordinate along cylinder liner,

h – nominal oil film thickness,
h_T – average separation,
p – hydrodynamic pressure,
u – axial piston velocity,
μ – oil dynamic viscosity,
$v=\partial h/\partial t$ – radial piston velocity,
σ – composite root-mean-square roughness of mating surfaces.

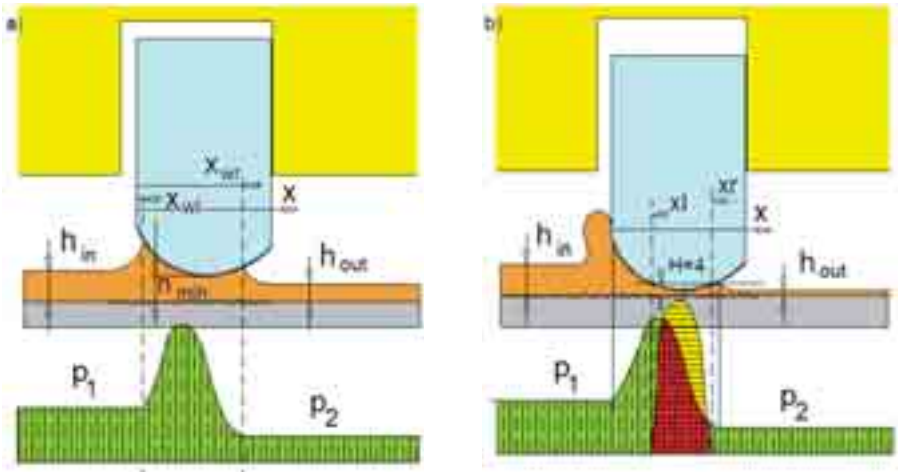

Fig. 3. Scheme of gap between the ring face and cylinder liner in the case of: a) hydrodynamic and b) mixed friction

The significance and mathematical description of empirical coefficients ϕ_x , ϕ_S and boundary conditions of equation (4) are presented in [7, 8] and also in [13].

The effects of interacting asperities of piston ring and cylinder liner surfaces were modelled using the mathematical model developed by Greenwood and Tripp [3], which was described in detail in publication [13] of the author of this article.

2.4. Model of ring torsional deformation and ring axial movement in the piston groove

A scheme of forces acting on a piston ring, action lines and distances between these forces and the centre of gravity ***S*** of the ring cross-section are shown in Fig. 4. All the forces are referenced to unit circumference of the piston ring (unit forces [N/m]).

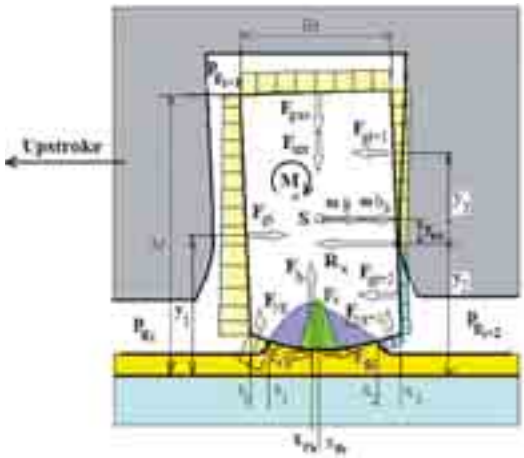

Fig. 4. Scheme and definitions of forces acting on a piston ring

Typical set of equations for the piston ring has the following form:

a) in radial direction:

$$\Sigma F_r = F_h + F_c + F_{yg_i} + F_{yg_{i+2}} - F_{spr} - F_{gas} = 0, \tag{5}$$

where:
F_h – hydrodynamic normal force,
F_c – elastic direct rough surface contact normal force,
F_{spr} – ring spring force,
F_{gas} – back ring gas force,
F_{ygi} – leading edge gas force,
F_{ygi+2} – trailing edge gas force.

b) in axial direction

$$\Sigma F_x = R_x - F_{fri} - F_{cx} + F_{g_{i+1}} + F_{g_{i+2}} - F_{g_i} - \frac{m}{c_{imc}}\left(g + b_k\right) = 0, \tag{6}$$

where:
R_x – groove reaction force,
F_{fri} – viscous friction force,
F_{cx} – contact friction force,
F_{gi+1}, F_{gi+2} – trailing side gas forces,
F_{gi} – leading side gas force,
m – ring mass,
g – gravitational acceleration,
b_k – piston acceleration,
c_{imc} – ring circumference.

Using these equations, one can calculate the reaction force $\boldsymbol{R_x}$ between the ring and piston groove in every time step. If the sign of this force changes, the axial movement of the ring in the piston groove begins. At this point, the value of the reaction force $\boldsymbol{R_x} = 0$ and the axial movement of the ring relative to the piston groove can be described by the following differential equation:

$$\frac{m}{c_{imc}}\frac{d^2 x_r}{dt^2} = -F_{fri} - F_{cx} + F_{g_{i+1}} + F_{g_{i+2}} - F_{g_i} - \frac{mg}{c_{imc}}. \tag{7}$$

The ring movement $\boldsymbol{x_r}$ completes when the ring reaches the opposite side of the piston groove.

The twist around the centre of gravity of the ring cross-section (point S in Fig. 4) can be described by the following equation of equilibrium of acting moments:

$$\Sigma M_S = F_h\left(x_S - x_{F_h}\right) + F_c\left(x_S - x_{F_c}\right) - \left(F_{fri} + F_{cx}\right)\frac{A_r}{2} - F_{g_i}\left(y_2 + y_{sc} - y_1\right) - F_{g_{i+1}}\left(y_3 - y_{sc}\right) +$$
$$+ F_{g_{i+2}}\left(\frac{y_2}{2} + y_{sc}\right) + R_x \cdot y_{sc} - K \cdot \theta = 0. \tag{8}$$

Estimating the ring torsional stiffness $\boldsymbol{K}$ as described in [14] and using the equation (8) of moment equilibrium, one can calculate the ring twist angle $\boldsymbol{\theta}$.

3. Experimental verification of developed models

A verification of the simulation model has been done by the author for a two-stroke marine Diesel engine [1, 9, 12]. The main data of the engine is presented in Tab. 1 (next chapter).

The experimental verification of the model of gas flow through the labyrinth seal of piston rings was carried out using measurements of unsteady gas pressure in the cylinder, between the piston rings and under piston performed by piezoelectric sensors mounted in the piston. A satisfactory qualitative and quantitative compatibility of the analyzed pressure variations has been achieved. The maximal relative differences between measured and calculated pressure values have not exceeded 15% [15, 18].

On the other hand, the experimental verification of the hydrodynamic model of piston rings involved measurement results of scraped oil volumes by a gland-box of a two-stroke marine engine. Unfortunately, similar measurements for piston ring packs of tested engines have not been carried out. Examination of scraped oil volumes by the ring pack (of the gland-box of marine internal combustion engine) proves a satisfactory quantitative agreement between numerical and experimental results. The maximal relative differences between measured and calculated values have not exceeded 10% [15, 18].

4. Calculation results

The simulation investigations have been done for a marine two-stroke Diesel engine designed at *Wärtsilä's* R&D engine centre in Switzerland. The main data of the engine is presented in Tab. 1. According to the request of the engine development company, the exact type of the engine has not been revealed.

Tab. 1. Main data of the marine engine under consideration

Cylinder bore [mm]	580
Piston stroke [mm]	2416
Engine rotational speed [rpm]	105

The type of ring set considered is common in marine engines. It consists of four rings with profiled sliding surfaces (Fig. 2 and 5). The package includes conventional straight ring end gaps. The surface geometry of the piston ring package, with vertical dimensions magnified by factor of 1000 relative to the horizontal ones, is depicted in Fig. 5. All the rings have the same asymmetrical barrel shape. In order to ensure very low wear of profiled surfaces, piston rings are coated (for example the top ring has chromium ceramic coating) [1, 9]. As a consequence, even hydrodynamic conditions during a long period of piston rings operation can be ensured.

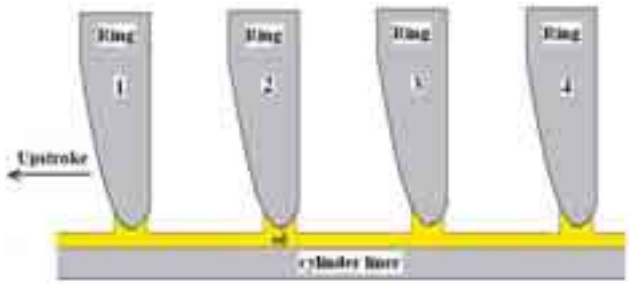

Fig. 5. Piston ring pack under consideration

In the previous papers of the author [15, 17, 18] computational and experimental results concerning piston-ring-cylinder system of a marine engine operating at full load have been described. In this paper, new calculation results for a part load range of a marine engine are presented.

The engine load can be characterised by several parameters (Tab. 2) like: achieved engine power, rotational speed, supercharging (scavenging) air pressure, etc. For the calculation, the lubricating oil consumption of 1 g/(kWh) [12] has been applied.

Tab. 2. Load parameters of marine engine under consideration

Engine load parameters	Engine load			
	25%	50%	75%	100%
Power [kW/cyl.]	531	1063	1594	2125
Rotational speed [rpm]	66	83	95	105
Scavenging air pressure [bar]	1.36	2.14	2.99	3.85

Typically, the figures that will follow show variation of some physical parameters as a function of the crankshaft rotation angle, beginning from the piston bottom dead centre (BDC) of the two-stroke engine operation (0°). In this case, the end of compression phase is at 180° of crank angle (piston top dead centre - TDC).

Figure 6 presents the gas pressure variations in cylinder versus crank angle for four values of engine load: 25%, 50%, 75% and 100%. More details concerning engine loads are shown in Tab. 2. For this purpose, a special computer programme concerning engine cycle calculation has been used. On the basis of known cylinder pressure variation and simulated gas leakage through the labyrinth sealing of the piston ring pack the gas pressures among piston rings have been also calculated [17, 18] (not shown in this paper). Generally, the gas pressure in the cylinder for all engine loads increase during the piston upstroke (compression phase) and decrease during a certain part of the piston downstroke (expansion phase). In Fig. 6, the following maximum gas pressure values in cylinder can be seen: 156 bar at 100% engine load, 141 bar (75% load), 112 bar (50% load) and 83 bar (25% load). The more engine load is achieved the higher maximal value of gas pressure in cylinder can be observed.

The higher is the gas pressure the stronger is the radial gas force acting to increase the ring diameter. It means that the radial gas force can be many times greater than the natural force due to ring stiffness acting in the same direction. First of all, the first ring (top ring) is strongly pressed against the cylinder liner surface. For this reason, the comparisons of computational results concerning different engine loads are presented for the first piston ring (Fig. 7-9 and 12).

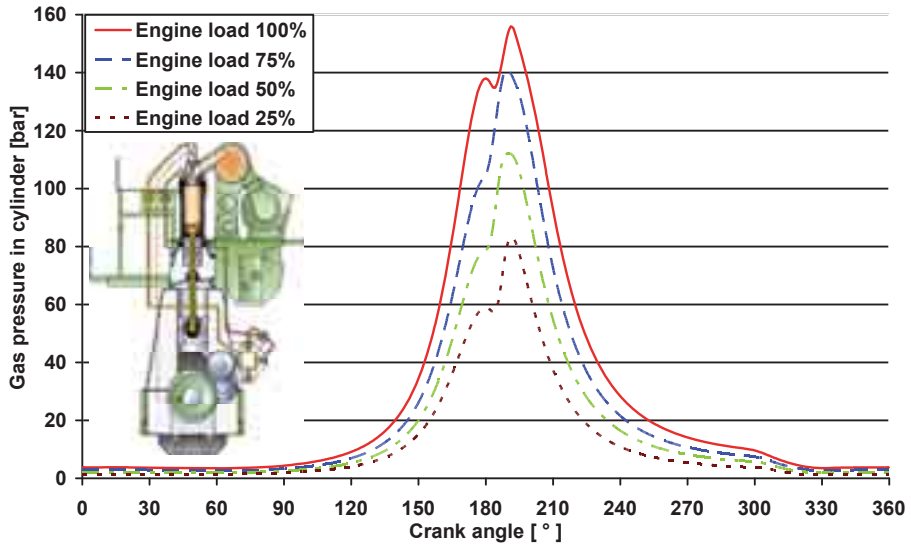

Fig. 6. Gas pressure variations in cylinder for different engine loads versus crankshaft rotation

In Fig. 7, ring lifts in piston grooves as a function of crank angle are shown. Gas pressure variations at the location of scavenging air ports are responsible for mostly short lasting lifts of the top piston ring during the piston upstroke. Much more important are ring lifts during the piston downstroke (expansion period). Due to gas pressure variations between piston rings, axial

movements of the top ring in piston groove can be observed, respectively in the range between 222° and 292° of crank angle at 100% engine load and between 222° and 284° of crank angle at 50% engine load. Axial inertial forces acting on piston rings are significantly less important for low-speed two-stroke marine engines than for four-stroke engines.

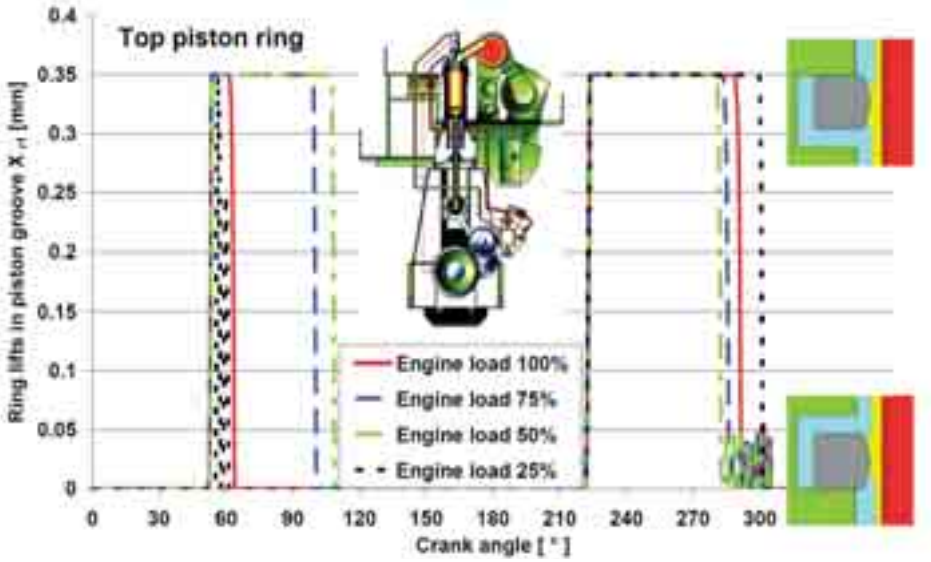

Fig. 7. Variation of ring lift X_{r1} in the first (top) piston groove for different engine loads versus crank angle

The nominal axial clearance of each ring in piston groove equals 0,35 mm. Each short lasting ring movement in the piston groove is followed by a change of the acting point of the reaction force R_x to the other flank of piston groove and also a sign change of this force (Fig. 4). Obviously, $R_x=0$ during the ring movement between the two piston groove flanks.

The total radial force acting on a piston ring compensates first of all the gas force F_{gas}, hydrodynamic force F_h , elastic contact force due to surface roughness F_c , spring force F_{spr} (see Fig. 4 and equation (5)). In Fig. 8, variations of total radial forces of the top piston ring for different engine loads versus crank angle are presented. They look similar to variations of gas pressures in cylinder (Fig. 6). The more engine load is achieved the higher maximal value of total radial force acting on the sliding surface of the top ring can be observed.

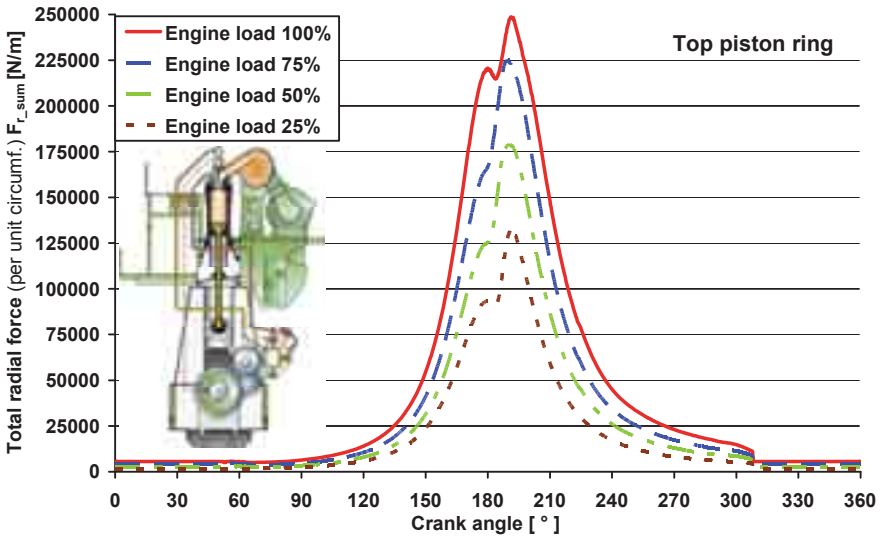

Fig. 8. Variation of total radial unit force (hydrodynamic and elastic contact) $F_{r\,sum}$ of the top piston ring for different engine loads versus crank angle

The total friction forces acting on piston rings consist of two tangential components: hydrodynamic and elastic contact forces due to surface roughness. Variations of these forces for the top piston ring as functions of crank angle are presented in Fig. 9.

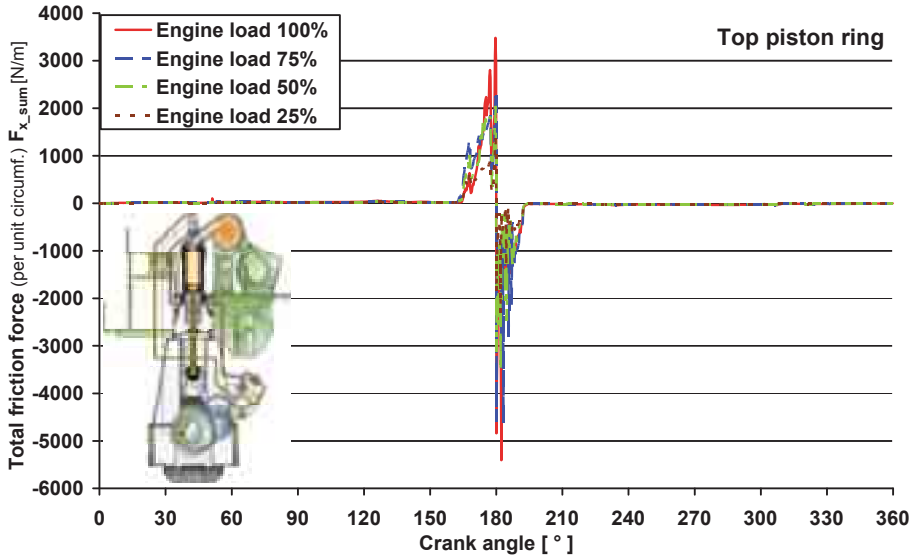

Fig. 9. Variation of total friction unit force $F_{x\,sum}$ for the top piston ring and different engine loads versus crank angle

The calculation results have been carried out for four chosen values of engine load: 25%, 50%, 75% and 100%. Hydrodynamic components of these forces (per unit of piston ring circumference) are much lower (50 N/m at full engine load) than components of elastic contact forces (4000 – 5000 N/m at full load). These mixed friction forces should be noticed near the top dead centre, where the highest gas pressure and oil temperature are reached. The sign change of these forces at TDC results from the sign change of piston velocity. The more engine load is achieved the higher value of total friction force acting on the sliding surface of the top piston ring can be observed.

Multiplying friction forces of all the rings by piston velocity, friction power losses can be calculated. In Fig. 10, variations of total power losses versus crank angle are presented. The higher engine load is achieved the more friction power loss is noticed.

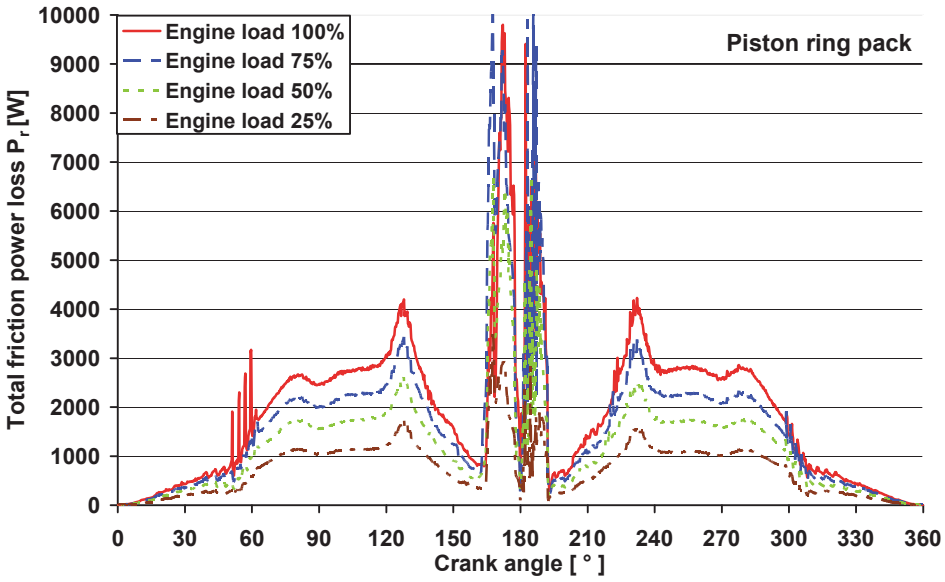

Fig. 10. Variation of total friction power loss P_r for different engine loads versus crank angle

The motion of the ring pack scraping and distributing oil on the cylinder liner leaves the oil film profiles shown in Fig. 11. Each profile corresponding to considered engine load is formed after a few cycles of operation. An uneven oil film distribution along the cylinder liner can be clearly seen. Low film thickness near the piston top dead centre (TDC) and in the other part of cylinder liner at the location of scavenging air ports should be noticed. The minimum oil film thickness at TDC is about 0.3 μm and is comparable with root mean square (RMS) roughness of the cylinder liner that equals 0.22 μm. The very low local film thickness values near TDC can be explained by occurrence of high gas pressure and high temperature in this area during the compression and working phases of engine operation. Due to high gas forces, piston rings are strongly pressed against the cylinder surface. On the other hand, high temperature reduces the oil viscosity. There are two places of oil supply for the cylinder liner of long-stroke IC engine located below TDC. Two peaks of oil film thickness at these places can be clearly seen in Fig. 11.

In a marine two-stroke engine, the location of scavenging air ports is also important for cylinder lubrication. Their presence simply reduces the mating surface between piston rings and cylinder liner. Due to low gas pressure and oil, temperature the greatest oil film thickness can be seen between scavenging air ports and bottom dead centre.

The higher engine load is achieved the more lubricating oil is supplied on cylinder liner surface, but the lower oil film thickness is left by the ring pack along cylinder wall.

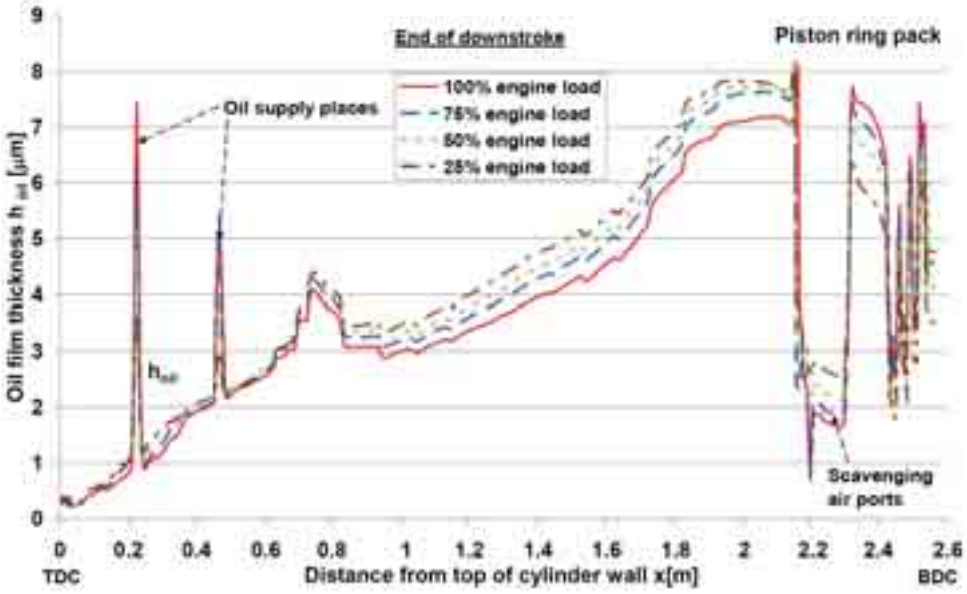

Fig. 11. Variation of the oil film thickness $\boldsymbol{h_{oil}}$ *left by the ring pack along cylinder wall for different engine loads*

The twist movement of piston rings should be taken into account if the lubrication problem of cylinder liner is studied. Maximum value of the twist angle of the top ring appears in the phase of piston motion corresponding to high gas pressure in the combustion chamber and reaches -5,6' (minute). The ring twists in such a way that the gap deformation causes the decrease of hydrodynamic force during upstroke and a higher amount of oil scraping to combustion chamber is observed [14].

Due to axial movements of the top piston ring, the resulting significant variations of ring twists can be observed (compare Fig. 7 and 12). In addition, sudden decrease of gas pressure at the location of scavenging air ports causes further substantial variations of ring twists.

The twist angle of the top ring slightly depends on engine load. Different twist angle variations in the range between 64° and 109° of crank angle (piston upstroke) mostly result from different crank angle values of the axial ring lift in piston groove (see Fig. 7).

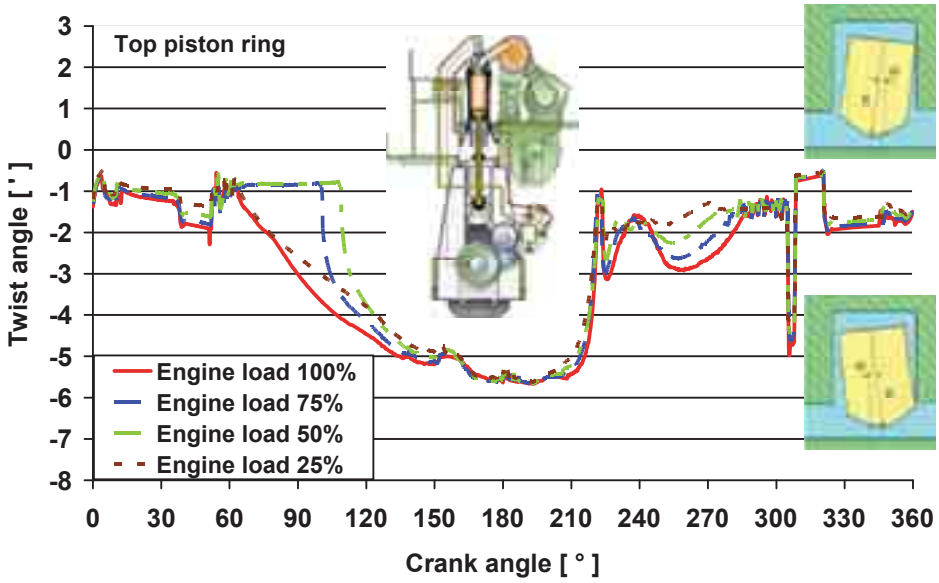

Fig. 12. Variation of twist angle Θ_1 of the top piston ring for different engine loads versus crank angle

5. Conclusions

The major conclusions that may be drawn from the results are as follows:

1. The developed mathematical model and simulation programme give a lot of practical information that would be more complicated and expensive to obtain using experimental methods.
2. In order to use the simulation programme a number of important input data (also experimental data) is needed. This mainly concerns the system piston – ring – cylinder, for example geometrical profiles of sliding surfaces of piston rings, thermal deformations of piston and cylinder, profiles of piston grooves, etc..
3. If more engine load is achieved then the following main phenomena can be noticed:
   a) higher gas pressure in cylinder,
   b) higher hydrodynamic and elastic contact force acting on the top piston ring,
   c) higher friction force acting on the top piston ring,
   d) more friction power loss of the piston ring pack,
   e) more lubricating oil is supplied on cylinder liner surface, but lower oil film is left by the ring pack along cylinder wall.
4. The main aim of simulation of piston rings operation is to predict lubrication conditions, define areas of the possible cylinder liner wear, determine changes of the shape of piston ring surface due to deformation and due to wear, and finally determine the gas leakage through the sealing ring set. Further investigation of these phenomena should be recommended.

Acknowledgements

The author expresses his gratitude to *Wärtsilä's* R&D engine centre in Winterthur (Switzerland) for having the opportunity to work on projects concerning mathematical modelling and numerical simulation of tribological systems of piston rings and gland-box during many research periods at this company.

References

[1] Demmerle, R., Barrow, S., Terrettaz, F., Jaquet, D., *New Insights into the Piston Running Behaviour of "Sulzer" Large Bore Diesel Engines,* CIMAC Congress, Hamburg 2001.

[2] Dowson, D., *Piston Assemblies; Background and Lubrication analysis,* Engine Tribology, Taylor C. M. (editor), Elsevier Science, pp. 213-240, 1993.
[3] Greenwood, J., Tripp, J.H., *The contact of Two Nominally Flat Rough Surfaces*, Proc I. Mech. E., Vol. 185, pp. 625-633, 1971.
[4] Iskra, A., *Parametry filmu olejowego w węzłach mechanizmu tłokowo – korbowego silnika spalinowego,* Wydawnictwo Politechniki Poznańskiej, Poznań 2001.
[5] Koszałka, G., Niewczas, A., Guzik, M., *Predicted and Actual Effect of Cylinder Liner Wear on the Blowby in a Truck Diesel Engine*, SAE Paper, No. 2008-01-1717, 2008.
[6] Koszałka, G., *Application of the piston-rings-cylinder kit model in the evaluation of operational changes in blowby flow rate,* Maintenance and Reliability, No. 4, pp. 72-81, 2010.
[7] Patir, N., Cheng, H. S., *An Average Flow Model for Determining Effects of Three-Dimensional Roughness on Partial Hydrodynamic Lubrication*, Transactions of ASME, Vol. 100, January 1978.
[8] Patir, N., Cheng, H.S., *Application of Average Flow Model to Lubrication Between Rough Sliding Surfaces*, Transactions of ASME, Vol. 101, April 1979.
[9] Räss, K., Amoser, M., *Progressive development of two-stroke engine tribology,* Paper No. 83, CIMAC Congress, Vienna 2007.
[10] Serdecki, W., *Badania współpracy elementów układu tłokowo – cylindrowego silnika spalinowego,* Wydawnictwo Politechniki Poznańskiej, Poznań 2002.
[11] Tian, T., *Dynamic Behaviors of Piston Rings and Their Practical Impact-Part II: Oil Transport, Friction, and Wear of Ring/Liner Interface and the Effects of Piston and Ring Dynamics*, Proc. Inst. Mech. Eng., Part J: Journal of Engineering Tribology, Vol. 216, pp. 229-247, 2002.
[12] *Wärtsilä Technology Review*, information materials concerning IC engines designed at *Wärtsilä* company.
[13] Wolff, A., Piechna, J., *Numerical simulation of piston ring pack operation in the case of mixed lubrication*, The Archive of Mech. Engineering, Vol. LII, No. 3, pp. 157-190, 2005.
[14] Wolff, A., Piechna, J., *Numerical simulation of piston ring pack operation with regard to ring twist effects,* The Archive of Mech. Engineering, Vol. LIV, No. 1, pp. 65-99, Warsaw 2007.
[15] Wolff, A., *Experimental verification of the model of piston ring pack operation of an internal combustion engine,* The Archive of Mechanical Engineering, Vol. LVI, No. 1, pp. 73-90, Warsaw 2009.
[16] Wolff, A., *Numerical analysis of piston ring pack operation,* Combustion Engines, No. 2, pp. 128-141, Poznań 2009.
[17] Wolff, A., *Modelowanie i symulacja numeryczna funkcjonowania pakietu pierścieni tłokowych dwusuwowego silnika okrętowego,* Zesz. Nauk. Inst. Pojazd., Wydz. Sam. i Masz. Robocz., Warsaw University of Technology, Z. 1 (82), pp. 5-17, Warsaw 2011.
[18] Wolff, A., *Numerical analysis of piston ring pack operation of a marine two-stroke engine,* Combustion Engines, No. 3/2011 (146), (article on CD enclosed to the periodical), Poznań 2011.